DALTON
FULL PAPER

Multi-modal bridging ligands; effects of ligand functionality, anion and crystallisation solvent in silver(I) co-ordination polymers †

Alexander J. Blake, Neil R. Champness,* Paul A. Cooke, James E. B. Nicolson and Claire Wilson

School of Chemistry, The University of Nottingham, University Park, Nottingham, UK NG7 2RD. E-mail: Neil.Champness@nottingham.ac.uk

Received 20th April 2000, Accepted 6th June 2000
First published as an Advance Article on the web 10th October 2000

The influence of solvent and anion on the formation of co-ordination polymers of silver(I) and the multi-modal ligands 2,2′-bipyrazine (bpyz) and pyrazino[2,3-*f*]quinoxaline (pyq) has been studied. Reaction of AgX (X = BF_4^- or PF_6^-) with bpyz or pyq in $MeNO_2$ affords three-dimensional co-ordination networks, $\{[Ag(bpyz)]X\}_\infty$ or $\{[Ag(pyq)]X\}_\infty$. Whereas $\{[Ag(bpyz)]X\}_\infty$ form diamond-like networks, which adopt a chiral structure due to the different bridging modes of the bpyz ligand, $\{[Ag(pyq)]X\}_\infty$ form unusual achiral three-dimensional frameworks which are constructed from bridged $[Ag(pyq)]_\infty$ tubes. In the case of $\{[Ag(bpyz)]X\}_\infty$ an increase in anion volume from BF_4^- to PF_6^- leads to a corresponding increase in helix volume and concomitant contraction of the helical pitch of the diamondoid framework. The use of co-ordinating solvents of crystallisation in the reactions of $AgBF_4$ with bpyz results in the formation of an undulating two-dimensional sheet, $\{[Ag(bpyz)(MeCN)]BF_4\}_\infty$, when MeCN replaces $MeNO_2$, or a one-dimensional polymer $\{[Ag_2(bpyz)_2(PhCN)][BF_4]_2\}_\infty$, when PhCN is used. Reaction of $AgBF_4$ with pyq in either MeCN or PhCN affords the discrete molecular complex $[Ag(pyq)_2]BF_4$ in which only the chelating donors of the pyq ligand are co-ordinated to the silver(I) ion. $[Ag(pyq)_2]BF_4$ exhibits dimorphism with the two structures observed differing in the nature of their π–π interactions.

Inorganic supramolecular chemistry and in particular the construction of polymeric co-ordination networks is an extremely topical area of research.[1,2] The construction of a wide variety of network topologies has been achieved through ligand design and the use of different transition metal co-ordination geometries.[1] These include one-dimensional chains,[2] which can be helical,[3,4] two-dimensional sheets with a variety of connectivities[5] and three-dimensional structures,[6] such as the diamondoid or adamantoid structures.[7,8] Such compounds can also exhibit other structural phenomena from simple guest inclusion[9] to interdigitation,[10] interpenetration[1] and even self-entanglement or polyknotting.[11]

The balance between the formation of different structures is often subtle. Factors that affect the co-ordination polymer topology include not only the highly influential forces of metal and ligand co-ordination preferences but also anion-based interactions and solvent effects. These latter factors are particularly notable in silver(I) co-ordination polymers.[12] Owing to the flexible co-ordination sphere of Ag^I, co-ordination numbers from two to six are all possible, and due to the relatively weak nature of many Ag^I–ligand interactions such compounds are particularly susceptible to the influence of weaker supramolecular forces.

Ligand design is often a useful way of manipulating the overall structural order. Many bidentate aromatic N–donor ligands, such as the archetypal 4,4′-bipyridyl, have been studied in this respect as donor separation and orientation, and steric and electronic properties can readily be controlled. We are now developing this type of ligand[13] so that we can gain further control over metal bridging by studying the properties of what we term multi-modal bridging ligands. Examples of such ligands are 2,2′-bipyrazine (bpyz) and pyrazino[2,3-*f*]quinoxaline (pyq) (Scheme 1). These ligands differ from more traditional tri- and tetra-dentate bridging ligands in that they offer the metal chemically distinct binding sites, both chelating and monodentate, and distinct bridging modes (Scheme 1). By using such ligands for co-ordination polymer construction we are introducing further control over network formation by inherently linking two bridging units in a controlled manner. Multi-modal ligands which have a similar combination of one chelating and two monodentate donor sites, namely 2,2′-bi-1,6-napthyridine and 5,5′-dicyano-2,2′-bipyridine, have previously been shown to generate unusual structures in the elegant work of Janiak and co-workers.[4]

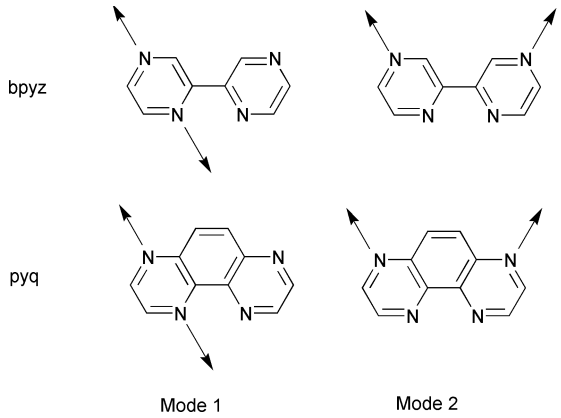

Scheme 1 Potential bridging modes for bpyz and pyq.

We have recently communicated aspects of this work and now report a more extensive study of the effects of solvent and anion in the construction of silver(I) co-ordination polymers with multi-modal ligands.[13]

† Based on the presentation given at Dalton Discussion No. 3, 9–11th September 2000, University of Bologna, Italy.

Electronic supplementary information (ESI) available: rotatable 3-D crystal structure diagram in CHIME format. See http://www.rsc.org/suppdata/dt/b0/b003202f/

DOI: 10.1039/b003202f

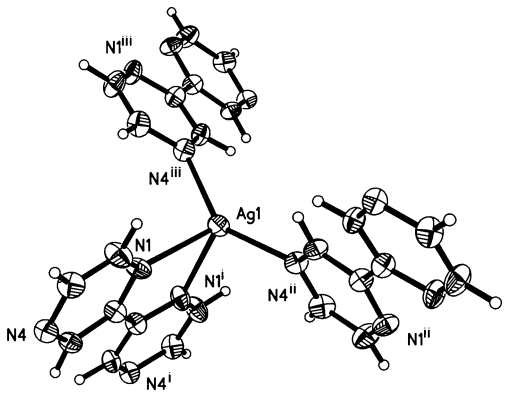

Fig. 1 View of the silver(I) geometry observed in complex **1** indicating the numbering scheme adopted in both **1** and **2**. The latter adopts the same silver(I) environment with minor variations in bond lengths and angles. Displacement ellipsoids are drawn at the 50% probability level. Symmetry codes: i $-y+1, -x+1, -z+\frac{1}{2}$; ii $-x+\frac{3}{2}, y+\frac{1}{2}, -z+\frac{3}{4}$; iii $-y+\frac{1}{2}, x-\frac{1}{2}, z-\frac{1}{4}$.

Results and discussion

Micro-crystalline powders of seven compounds have been prepared by the reaction of either 2,2′-bipyrazine (bpyz) or pyrazino[2,3-*f*]quinoxaline (pyq) with AgX (X = BF_4^- or PF_6^-) in $MeNO_2$, MeCN or PhCN followed by precipitation with diethyl ether. To aid structural comparisons single crystals of all the complexes were grown by diffusion of diethyl ether vapour into solutions of the complexes, prepared by slow mixing of the silver(I) salt and ligand in the appropriate solvent. In all cases crystals of only a single morphology grew from a given reaction solution.

The single crystal structures of both ligands used in this study were determined in order to compare the degree of π–π interactions in the "free" ligands and that observed in the complexes. The structure of bpyz shows that the ligand adopts a planar structure with the two pyrazine rings related to each other by an inversion centre. As a result the ligand adopts an arrangement such that the two central nitrogen atoms are placed *anti* to each other as observed in the structure of 2,2′-bipyridyl.[14] The bpyz molecules are stacked with a ring centroid to plane separation of 3.36 Å representing a significant π–π interaction. The structure of pyq similarly exhibits π–π interactions within columns of pyq molecules in this case with a centroid–plane separation of 3.34 Å, similar to the intermolecular distance observed in the structure of 1,10-phenanthroline.[15]

Structures of $\{[Ag(bpyz)]BF_4\}_\infty$ 1 and $\{[Ag(bpyz)]PF_6\}_\infty$ 2

The complexes $\{[Ag(bpyz)]BF_4\}_\infty$ **1**[13] and $\{[Ag(bpyz)]PF_6\}_\infty$ **2** both crystallise in the chiral tetragonal space group $P4_32_12$ and adopt both the same silver(I) co-ordination environment and topological arrangement. The Ag^I ion is co-ordinated by one chelating ligand and by two monodentate N-donors from two further bpyz ligands in a distorted tetrahedral geometry (Fig. 1) (Table 1). Each Ag^I is linked to four nearest-neighbour silver(I) centres, two *via* the chelating ligand and two more through two peripheral monodentate N-donors forming a distorted diamondoid array (Fig. 2). Inspection of the extended lattice viewed down the *c* axis shows that the structure forms two distinct channels which represent different helices running through the network (Fig. 3). The square-shaped channel, A, runs through a 4_3 helix in which each Ag^I is linked to the next along the helix through bridging mode 1 (Scheme 1). In contrast, the rhomboid-shaped channel, B, runs through a 2_1 helix in which adjacent Ag^I ions are linked through bridging mode 2 (Scheme 1) *via* two peripheral N-donors (Fig. 4). Whereas in a conventional diamondoid lattice adjacent helices which have opposing hands are chemically identical, in **1** and **2** adjacent anti-parallel helices are chemically distinct, displaying different bridging modes which result in overall chirality in the structures. Rectangular channels also run through the structure

Table 1 Selected bond lengths (Å) and angles (°) for compounds **1** and **2**

1		**2**	
Ag1–N1	2.425(7)	Ag1–N1	2.377(2)
Ag1–N1^{i}	2.425(7)	Ag1–N1^{iv}	2.377(2)
Ag1–N4^{ii}	2.223(8)	Ag1–N4^{v}	2.240(2)
Ag1–N4^{iii}	2.223(8)	Ag1–N4^{vi}	2.240(2)
N1^{i}–Ag1–N1	69.2(3)	N1^{iv}–Ag1–N1	70.45(10)
N4^{ii}–Ag1–N1	105.9(3)	N4^{v}–Ag1–N1	98.87(8)
N4^{iii}–Ag1–N1	104.0(3)	N4^{vi}–Ag1–N1	117.38(7)
N4^{ii}–Ag1–N1^{i}	104.0(3)	N4^{v}–Ag1–N1^{iv}	117.38(7)
N4^{iii}–Ag1–N1^{i}	105.9(3)	N4^{vi}–Ag1–N1^{iv}	98.87(8)
N4^{ii}–Ag1–N4^{iii}	143.6(4)	N4^{vi}–Ag1–N4^{v}	135.85(11)

Symmetry transformations used to generate equivalent atoms: i $-y+1, -x+1, -z+\frac{1}{2}$; ii $-x+\frac{3}{2}, y+\frac{1}{2}, -z+\frac{3}{4}$; iii $-y+\frac{1}{2}, x-\frac{1}{2}, z-\frac{1}{4}$; iv $y,x,-z$; v $-y+\frac{3}{2}, x+\frac{1}{2}, z-\frac{1}{4}$; vi $x+\frac{1}{2}, -y+\frac{3}{2}, -z+\frac{1}{4}$.

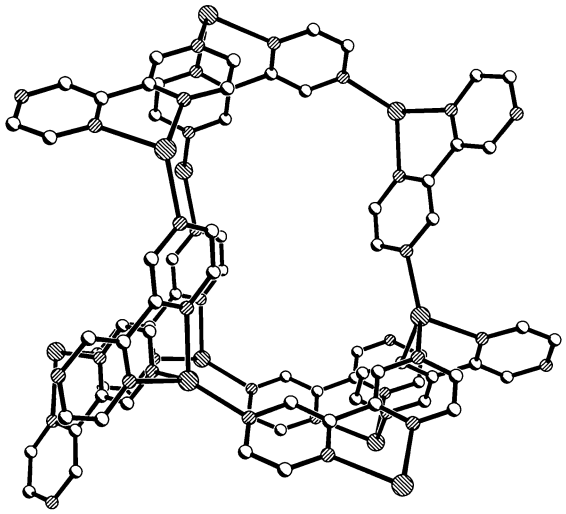

Fig. 2 View of a distorted adamantane-shaped unit within the structure of complex **1**. Hydrogen atoms are omitted for clarity (silver, left hatch; nitrogen, right hatch).

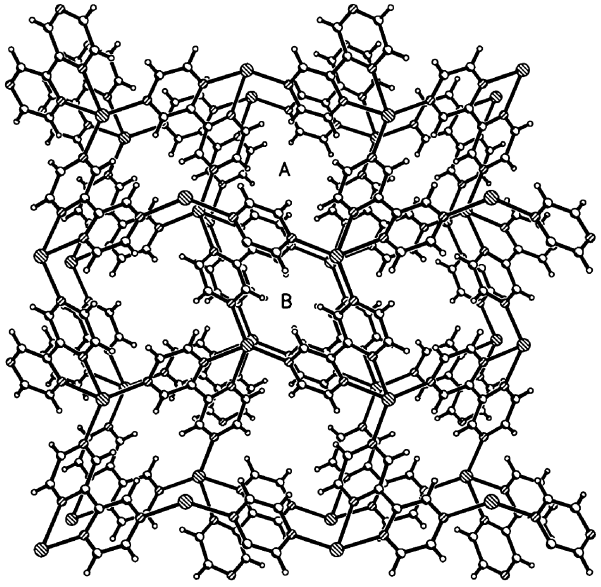

Fig. 3 Compound **2** viewed down the *c* axis showing the two channels A and B formed by the 4_3 and 2_1 helices respectively. Anions and guest solvent molecules are omitted for clarity (silver, left hatch; nitrogen, right hatch).

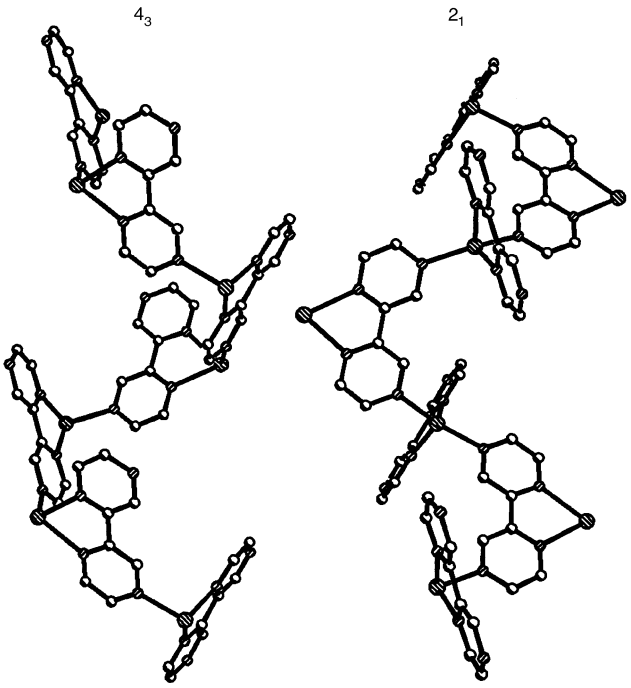

Fig. 4 Views perpendicular to channels A and B in complex **2** illustrating the 4_3 helix formed *via* bridging mode 1 and the 2_1 helix formed by bridging mode 2. Hydrogen atoms are omitted for clarity (silver, left hatch; nitrogen, right hatch).

parallel to the *a* and *b* axes (channel dimensions *ca.* 6 × 10 **1**, 7 × 9 Å **2**). The channels are filled by the counter anions and $MeNO_2$ solvent molecules. The solvent occupies 45.2% of the total crystal volume in the case of **1** and 41.1% in the case of **2**.[16] In both **1** and **2** the anions sit in channel B surrounded by the 2_1 helix leaving channel A (4.9 **1**, 4.1 Å **2** approximate cross-sections) to accommodate the guest solvent molecules.

Structure of $\{[Ag(pyq)]BF_4\}_\infty$ 3

Reaction of $AgBF_4$ with pyq in $MeNO_2$ also affords a three-dimensional co-ordination network. In this case three distinct silver(I) ions are found in the crystallographic asymmetric unit (Fig. 5). All three silver centres adopt a similar co-ordination geometry involving three pyq ligands, one chelating and two monodentate, to give a distorted tetrahedral geometry similar to that observed in compounds **1** and **2**. The geometries at all of the silver ions are similar with the smallest N–Ag–N angle between the two chelating N-donors as expected (Table 2). The angles between the N-donors of the chelating ligand and those of the monodentate ligands form two distinct units at each silver. One monodentate ligand adopts small angles (*ca.* 90–110°) between its N-donor and the chelating N-donors while the other monodentate donor atom forms larger angles (*ca.* 120–140°) with the neighbouring chelating ligand. The distortions observed in compound **3** result in the formation of an unusual three-dimensional structure which differs considerably from that observed for the analogous bpyz complexes. Although each Ag^I ion is linked *via* pyq ligands to four nearest-neighbour silver(I) junctions and each junction of the framework is tetrahedral, the structure observed for **3** is not diamondoid, as is the case for compounds **1** and **2**. The structures can be viewed as being constructed from inter-linked tubular units which run parallel to the *b* axis (Fig. 6). These tubular components are reminiscent of the periphery of the 4_3 helices formed in **1** and **2** with the exception that in this case the helices are internally linked to give a tubular motif. These tubes are in turn linked through bridging mode 1 in the [−1 0 1] direction and through mode 2 in the [101] direction giving rise to the three-dimensional structure observed (Fig. 7). Three distinct channels, C (*ca.* 3.4 Å cross-section), D (channel

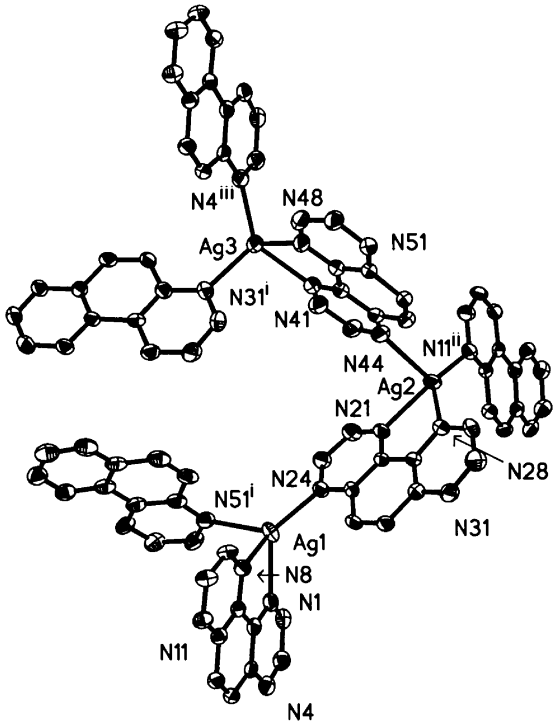

Fig. 5 The silver(I) environments observed in complex **3**, showing the numbering scheme adopted. Hydrogen atoms are omitted for clarity. Displacement ellipsoids are drawn at the 50% probability level. Symmetry codes: i $-x+\frac{3}{2}, y-\frac{1}{2}, -z+\frac{1}{2}$; ii $x-\frac{1}{2}, \frac{1}{2}-y, z-\frac{1}{2}$; iii $x-1, y, z$.

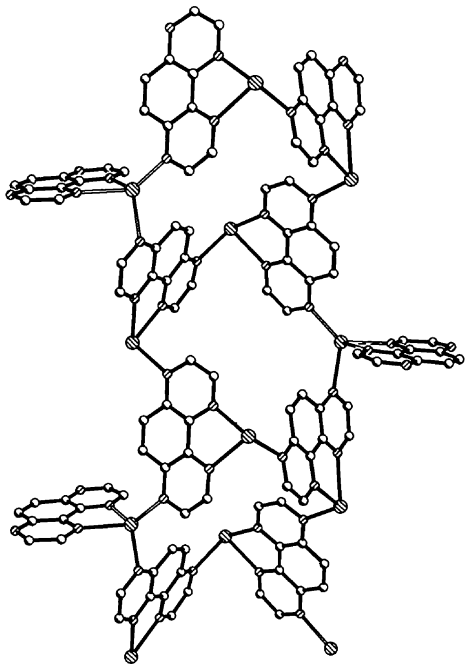

Fig. 6 View of the tubular units formed in complex **3** showing how the helix, reminiscent of the 4_3 helix observed in **1** and **2**, is interlinked by the silver(I) cations distinguished by open bonds. Hydrogen atoms are omitted for clarity (silver, left hatch; nitrogen, right hatch).

dimensions *ca.* 6 × 4.5 Å) and E (*ca.* 3.3 Å cross-section), running parallel to the *b* axis are filled by counter anions and guest $MeNO_2$ solvent molecules in the case of C and D but only by $MeNO_2$ molecules in the case of E. The solvent molecules account for 24.2% of the total crystal volume.[16] Single crystal diffraction experiments were performed on **4** but unfortunately we were unable satisfactorily to model extremely disordered anions and solvent molecules. However, we were able to identify that the cationic framework was topologically identical to that observed for **3**. It can also be concluded from the unit cell

Table 2 Selected bond lengths (Å) and angles (°) for compound **3**

Ag1–N24	2.202(5)	Ag2–N21	2.377(5)
Ag1–N51^{i}	2.362(5)	Ag2–N44	2.406(5)
Ag1–N1	2.376(5)	Ag3–N4^{iii}	2.232(5)
Ag1–N8	2.406(5)	Ag3–N31^{i}	2.320(5)
Ag2–N11^{ii}	2.213(5)	Ag3–N41	2.341(5)
Ag2–N28	2.284(5)	Ag3–N48	2.493(5)
N24–Ag1–N51^{i}	127.7(2)	N11^{ii}–Ag2–N44	105.0(2)
N24–Ag1–N1	130.6(2)	N28–Ag2–N44	109.1(2)
N51^{i}–Ag1–N1	96.0(2)	N21–Ag2–N44	88.7(2)
N24–Ag1–N8	123.2(2)	N4^{iii}–Ag3–N31^{i}	122.7(2)
N51^{i}–Ag1–N8	89.9(2)	N4^{iii}–Ag3–N41	134.2(2)
N1–Ag1–N8	71.1(2)	N31^{i}–Ag3–N41	102.6(2)
N11^{ii}–Ag2–N28	138.2(2)	N4^{iii}–Ag3–N48	105.7(2)
N11^{ii}–Ag2–N21	132.0(2)	N31^{i}–Ag3–N48	98.9(2)
N28–Ag2–N21	72.5(2)	N41–Ag3–N48	70.0(2)

Symmetry transformations used to generate equivalent atoms: i $-x+\frac{3}{2}, y-\frac{1}{2}, -z+\frac{1}{2}$; ii $x-\frac{1}{2}, \frac{1}{2}-y, z-\frac{1}{2}$; iii $x-1, y, z$.

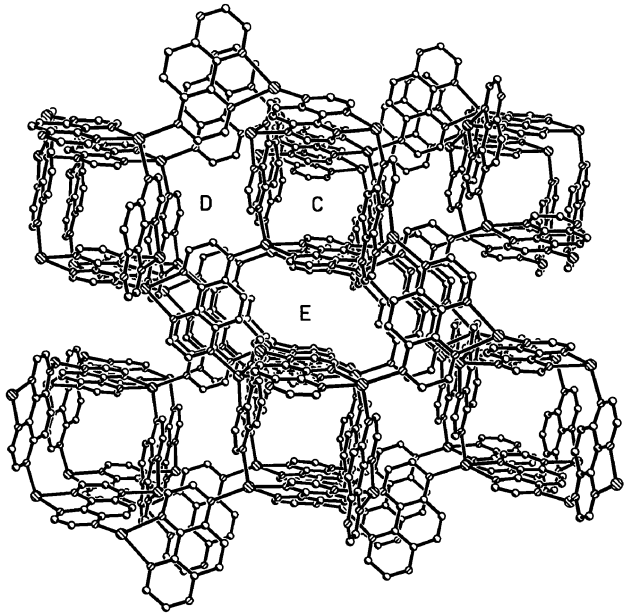

Fig. 7 View of the extended lattice formed by complex **3** down the *b* axis illustrating the tubular units, C, which are inter-linked forming two further types of channel D and E. Anions, guest solvent molecules and hydrogen atoms are omitted for clarity (silver, left hatch; nitrogen, right hatch).

dimensions for **3** and **4** that the change in anion has little effect upon the three-dimensional co-ordination network structure.

Structures of {[Ag(bpyz)(MeCN)]BF_4}$_\infty$ 5, {[Ag_2(bpyz)$_2$(PhCN)]-[BF_4]$_2$}$_\infty$ 6, [Ag(pyq)$_2$]BF_4 7

The effect of solvent upon the products obtained from the reaction of $AgBF_4$ with either bpyz or pyq was investigated by replacing $MeNO_2$ as the crystallisation solvent with the comparatively co-ordinating MeCN, or PhCN. Reaction of $AgBF_4$ with bpyz in MeCN afforded the product {[Ag(bpyz)(MeCN)]-BF_4}$_\infty$ **5**.[13] In this case each Ag^I co-ordinates a MeCN ligand in addition to three bpyz ligands, two monodentate and one chelating, leading to a distorted trigonal-bipyramidal geometry (Fig. 8a) (Table 3). Each Ag^I is linked through one chelating and two monodentate bpyz ligands to four nearest-neighbour silver(I) junctions as in **1** and **2**. However, in this case the co-ordination of the MeCN ligand flattens the extended lattice to give a two-dimensional (4,4) sheet (Fig. 9a). The MeCN co-ordination results in undulation of the sheets, with the MeCN ligands protruding from the surface which in turn results in interdigitation of adjacent {[Ag(bpyz)(MeCN)]BF_4}$_\infty$ layers (Fig. 9b). The five-co-ordinate geometry observed here is rare

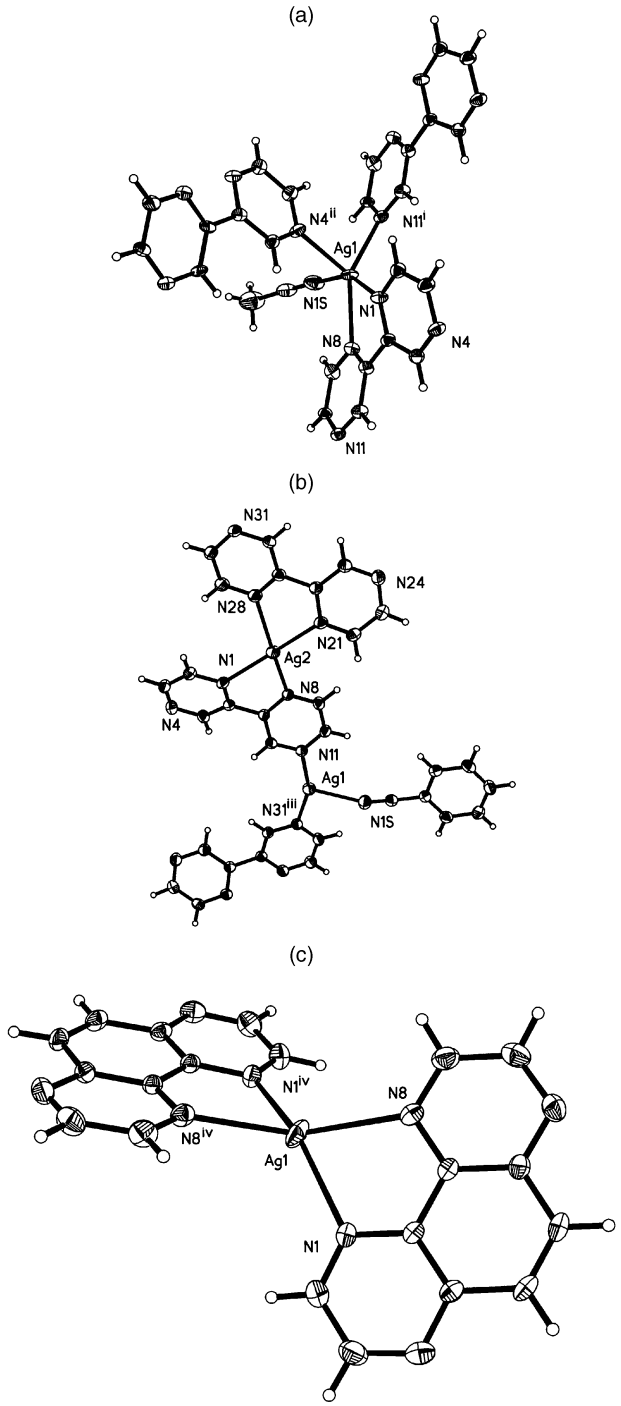

Fig. 8 View of the silver(I) environments observed in complexes **5** (a), **6** (b) and **7a** (c) indicating the numbering schemes adopted. The same numbering scheme was adopted for **7b**. Displacement ellipsoids are drawn at the 50% probability level. Symmetry codes: i $x-1, y, z$; ii $x-\frac{1}{2}, -y+\frac{3}{2}, z-\frac{1}{2}$; iii $1+x, \frac{3}{2}-y, z-\frac{1}{2}$; iv $-x-1, y, -z+\frac{1}{2}$; v $1-x, y, -z+\frac{1}{2}$.

for Ag^I, which prefers linear or tetrahedral co-ordination and has only been observed on three previous occasions in co-ordination networks.[17]

Replacing MeCN with PhCN as crystallisation solvent in the reaction of $AgBF_4$ with bpyz results in further changes in the extended structure with a quite different one-dimensional co-ordination polymer being isolated in this case. Single crystal X-ray diffraction studies showed that two distinct silver(I) environments are observed in the product {[Ag_2(bpyz)$_2$(PhCN)]-[BF_4]$_2$}$_\infty$ **6** (Fig. 8b). One Ag^I is co-ordinated in a distorted square-planar geometry (Table 3) by two chelating bpyz ligands (15.5° angle between the planes described by the two bpyz ligands) while the other links these [Ag(bpyz)$_2$]$^+$ units *via*

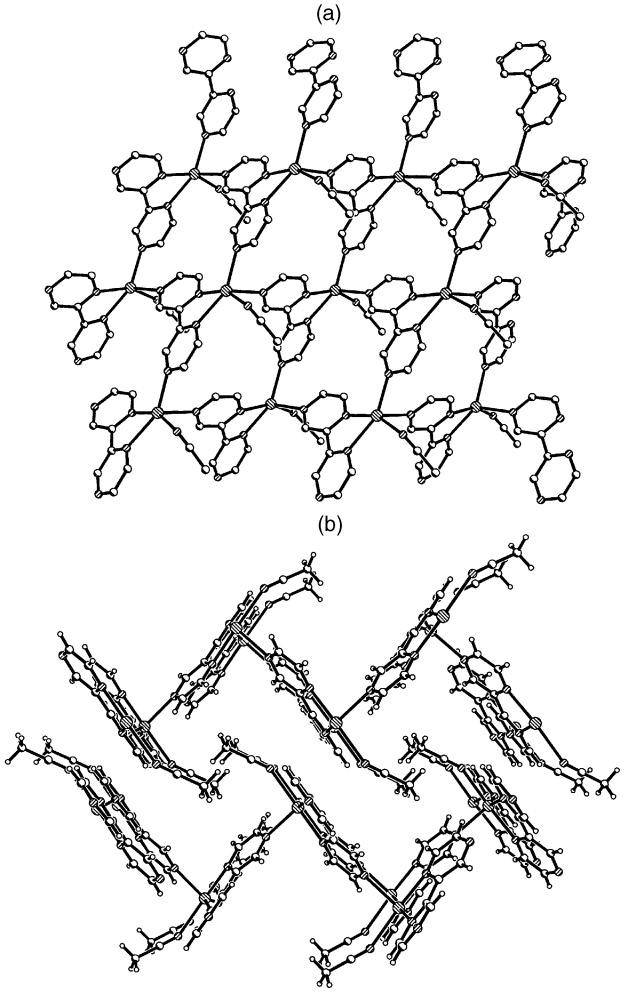

Fig. 9 (a) View of the (4,4)-two-dimensional sheet formed by complex **5**. Hydrogen atoms and anions are removed for clarity; (b) View perpendicular to the undulating sheets showing the interdigitation exhibited by the MeCN molecules on adjacent sheets. Anions are omitted for clarity (silver, left hatch; nitrogen, right hatch).

co-ordination of one peripheral monodentate bpyz donor per ligand. The second silver(I) environment adopts a distorted trigonal planar geometry with the third co-ordination site occupied by a PhCN ligand and the Ag^{I} ion sitting 0.039 Å from the plane formed by the three N-donor atoms (Table 3). The planar ribbons associate into sheets *via* π–π interactions between the PhCN ligand and one half of a bpyz ligand (centroid–plane separation = 3.30 Å) (F in Fig. 10) and between two bpyz aromatic ligands (centroid-plane separation = 3.25 Å) (G in Fig. 10) on adjacent ribbons. These interactions compare with a separation of 3.36 Å in the unco-ordinated ligand.

Reaction of $AgBF_4$ with pyq in a 1:1 or 1:2 reaction stoichiometry, in either MeCN or PhCN, affords the discrete, mononuclear, complex $[Ag(pyq)_2]BF_4$ **7** (Fig. 8c). It has been structurally characterised by single crystal X-ray diffraction experiments when crystals have been grown from MeCN (**7a**) or PhCN (**7b**) revealing that the compound exhibits dimorphism. In both cases the Ag^{I} adopts a distorted tetrahedral geometry (Table 3) and is co-ordinated exclusively by the chelating units of the pyq ligands. Complexes **7a** and **7b** differ predominantly in their packing modes although there are small differences in bond lengths and angles at the Ag^{I} and in the angle formed between the planes of the two pyq ligands (52.8 **7a**, 41.4° **7b**). In the case of **7a** $[Ag(pyq)_2]^+$ cations and BF_4^- anions are stacked such that the anions sit above and below the metal cation with Ag···F separations of 3.028(1) and 3.078(1) Å, respectively (Fig. 11a). The resultant chains are then interleaved *via* π–π interactions between pyq ligands on adjacent cations (plane–

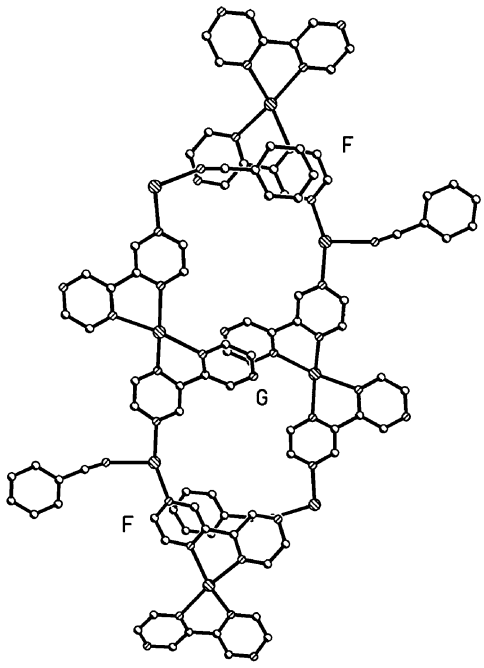

Fig. 10 View of the π–π interactions adopted between PhCN ligands and a bpyz ligand, F, and between two bpyz ligands, G, in complex **6**. Anions and hydrogen atoms are omitted for clarity (silver, left hatch; nitrogen, right hatch).

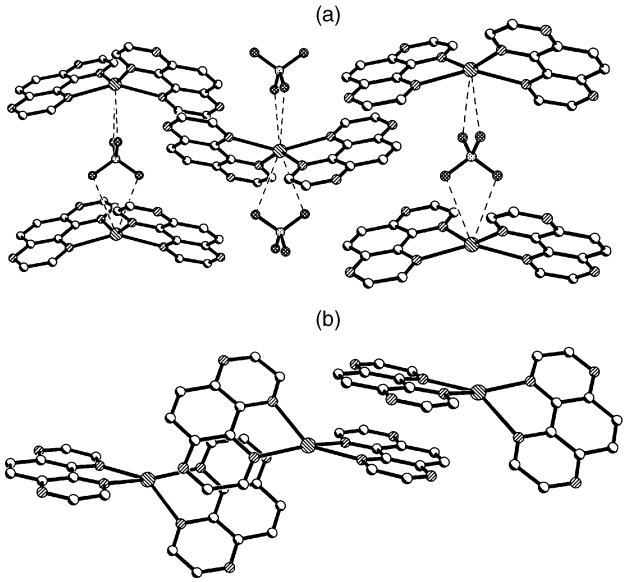

Fig. 11 (a) $Ag^{I}\cdots F_2BF_2$ and π–π interactions leading to the formation of two-dimensional sheets in complex **7a**, and (b) π–π interactions between adjacent $[Ag(pyq)_2]^+$ cations resulting in one-dimensional chains in **7b**. Hydrogen atoms, and anions in (b), are omitted for clarity (silver, left hatch; nitrogen, right hatch; fluorine, cross-hatched).

centroid distance = 3.25 and 3.26 Å). This results in the formation of sheets including both $[Ag(pyq)_2]^+$ cations and BF_4^- anions which run parallel to the [101] plane (Fig. 11a). In contrast **7b** packs in a different manner with no close contact between the Ag^{I} and the BF_4^- anions. Instead chains of $[Ag(pyq)]^+$ cations are formed, again *via* π–π interactions (plane–centroid distance = 3.33 Å), and run parallel to the *c* axis (Fig. 11b). These π–π interactions are generally shorter than those observed in the structure of the unco-ordinated ligand (3.34 Å), particularly in the case of **7a**, indicating an increased interaction upon co-ordination.

The structures of both complexes **7a** and **7b** contrast with that observed for the analogous NO_3^- salt $[Ag(pyq)_2]NO_3$ [18] which

Table 3 Selected bond lengths (Å) and angles (°) for compounds **5**–**7**

5		**6**		**7a**		**7b**	
Ag1–N11^{i}	2.345(6)	Ag1–N11	2.196(3)	Ag1–N1	2.3723(12)	Ag1–N1^{v}	2.2989(18)
Ag1–N1	2.394(6)	Ag1–N31^{iii}	2.214(3)	Ag1–N1^{iv}	2.3723(12)	Ag1–N1	2.2990(18)
Ag1–N8	2.404(6)	Ag1–N1S	2.444(3)	Ag1–N8^{iv}	2.3870(12)	Ag1–N8	2.4157(19)
Ag1–N4^{ii}	2.435(6)	Ag2–N8	2.318(3)	Ag1–N8	2.3870(12)	Ag1–N8^{v}	2.4157(19)
Ag1–N1S	2.467(7)	Ag2–N28	2.351(3)				
		Ag2–N21	2.360(3)	N1–Ag1–N1^{iv}	148.15(6)	N1–Ag1–N1^{v}	134.42(9)
		Ag2–N1	2.414(3)	N1^{iv}–Ag1–N8	117.93(4)	N1^{v}–Ag1–N8	146.23(6)
				N1^{iv}–Ag1–N8^{iv}	71.17(4)	N1–Ag1–N8	71.95(6)
N11^{i}–Ag1–N1	112.6(2)	N11–Ag1–N31^{iii}	157.94(10)	N1–Ag1–N8	71.17(4)	N1^{v}–Ag1–N8^{v}	71.95(6)
N11^{i}–Ag1–N8	146.1(2)	N11–Ag1–N1S	109.35(10)	N1–Ag1–N8^{iv}	117.92(4)	N1–Ag1–N8^{v}	146.23(6)
N1–Ag1–N8	69.0(2)	N31^{iii}–Ag1–N1S	92.58(10)	N8–Ag1–N8^{iv}	149.23(6)	N8–Ag1–N8^{v}	95.39(9)
N11^{i}–Ag1–N4^{ii}	89.0(2)	N8–Ag2–N28	157.24(10)				
N1–Ag1–N4^{ii}	91.6(2)	N8–Ag2–N21	114.27(9)				
N8–Ag1–N4^{ii}	124.9(2)	N28–Ag2–N21	71.08(9)				
N11^{i}–Ag1–N1S	90.0(2)	N8–Ag2–N1	71.26(9)				
N1–Ag1–N1S	155.9(2)	N28–Ag2–N1	106.96(9)				
N8–Ag1–N1S	87.6(2)	N21–Ag2–N1	170.53(9)				
N4^{ii}–Ag1–N1S	97.5(2)						

Symmetry transformations used to generate equivalent atoms: i $x-1$, y,z; ii $x-\frac{1}{2}$, $-y+\frac{3}{2}$, $z-\frac{1}{2}$; iii $1+x$, $\frac{3}{2}-y$, $z-\frac{1}{2}$; iv $-x-1$,y, $-z+\frac{1}{2}$; v $1-x$,y, $-z+\frac{1}{2}$.

similarly forms a discrete $[Ag(pyq)_2]^+$ cation but in this case the anion forms a much stronger bidentate interaction (Ag–O 2.541(10), 2.656(16) Å)[18] with the Ag^{I}, resulting in a distorted octahedral co-ordination geometry. As a result of the anion co-ordination the two pyq ligands adopt a *cis* arrangement.

Comparison of structures

Anion effects. It has previously been shown that the anion can have dramatic effects upon the long range order of co-ordination networks constructed from silver(I) salts and bridging N-donor ligands.[12] Diamondoid networks comprise helices and it can be seen in the studies by Moore and co-workers on $\{[AgL_2]X\}_\infty$ (L = 4,4′-biphenyldicarbonitrile; X = PF_6^-, AsF_6^- or SbF_6^-) that an increase in anion volume gives rise to either helix pitch elongation or lateral helical expansion.[8] This relatively simple explanation of pitch variation based upon anion volume can be extended to compounds **1** and **2** in the current study. Upon changing anion from BF_4^- (**1**) to PF_6^- (**2**) the pitch of both the 2_1, and consequently the 4_3, helices actually decreases from 13.80 to 11.02 Å. Inspection of the anion environments in **1** and **2** illustrates how helix pitch contraction takes place (Fig. 12). It can be seen that introduction of the larger PF_6^- anion (Fig. 12b) gives rise to movement of the neighbouring chelating bpyz ligands (indicated by open bonds) which in turn requires a twist of the next bpyz ligand along the 2_1 helix, in order to maintain the pseudo-tetrahedral silver(I) geometry, resulting in contraction of the pitch of the 2_1 helix.

The decrease in helix pitch upon increase of anion volume (38 BF_4^-, 54 Å^3 PF_6^-)[19] is in agreement with the observations of Moore and co-workers on the basis of helix volume variation.[8] The reduction of helix pitch upon changing anion from BF_4^- to PF_6^- is accompanied by an increase in the helix diameter (Scheme 2) (defined as the Ag···Ag separation perpendicular to the axis of the helix;‡) (3.52 **1**, 5.69 Å **2**) and thus an overall increase in the 2_1 helix volume (*ca.* 130 **1**, 280 Å^3 **2**). Thus the relationship between anion volume and helix volume is maintained. The 4_3 helices in the two compounds are less dramatically affected by the anion variation, as would be expected since the anions sit exclusively within the 2_1 helices. In this case there is only a small variation in the helix diameter (9.25 **1**, 9.68 Å **2**) resulting in a lower helical volume for **2** (*ca.* 930 **1**, 810 Å^3 **2**). Thus the increase in the volume of the 2_1 helix in **2** is compensated for by a decrease in the volume of the 4_3 helix resulting in a similar unit cell volume for **1** and **2**.

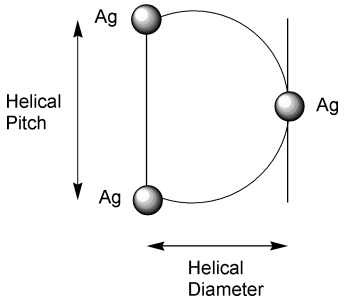

Scheme 2 The dimensions adopted for assessing helical volumes in complexes **1** and **2**.

Variation of the anion in the pyq complexes **3** and **4** results in less significant changes in the cationic network structure. Owing to the highly disordered nature of the anions and solvent molecules in the channels in **4** it is difficult to identify precisely the reason for the similarity of the cationic structures. However, this is perhaps explained by the fact that the anions sit within channels that also contain $MeNO_2$ solvent molecules, possibly minimising the direct impact of the anion volume variation.

Solvent effects. It can be seen from the structures of compounds **5** to **7** that the solvent used in crystallisation experiments has a gross effect upon the product isolated from the reaction of either ligand with $AgBF_4$. When non-co-ordinating $MeNO_2$ is used as the crystallisation solvent the silver(I) ions are ligated exclusively by bpyz, or pyq, donors as expected. However introducing co-ordinating solvents introduces potential competition for these ligands.

Introduction of a co-ordinating nitrile solvent allows effective solvation of Ag^+ cations in the form of $[Ag(MeCN)_4]^+$ or $[Ag(PhCN)_4]^+$ which are stable species.[20] Stabilisation of the cations provides competition for bpyz or pyq N-donors and it can be seen in the case of pyq that only a chelating interaction between cation and ligand is sufficiently favourable to displace solvent ligands and so form the bis-chelated discrete complex $[Ag(pyq)_2]BF_4$ **7**. In this case it seems apparent that the peripheral N-donors of the pyq ligands are relatively poor ligands in comparison to MeCN or PhCN, presumably due to their relatively hindered environments, and therefore will not displace the nitrile ligands from solvated silver(I) ions.

The peripheral N-donors of bpyz are less hindered and as a result provide a more competitive donor for silver(I) co-

‡ The definition of the diameter of the helix is somewhat arbitrary in the case of the 2_1 helix but the Ag···Ag separation has been chosen as an easily recognisable peripheral point of the helix.

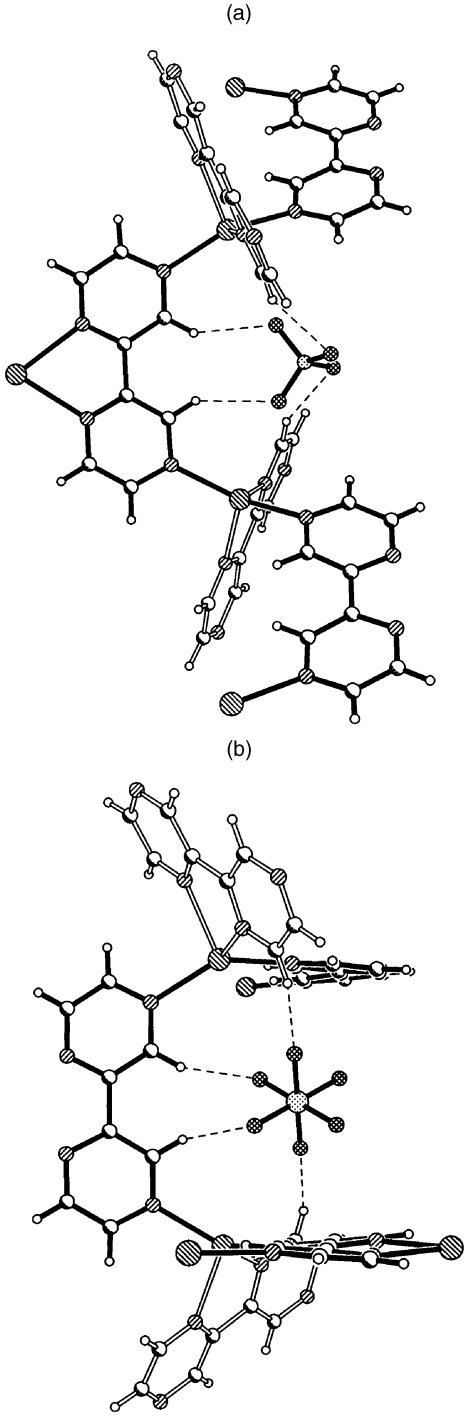

Fig. 12 Views perpendicular to channel B in compexes **1** (a) and **2** (b) indicating how the increased volume of the PF_6^- anion results in a decreased pitch of the 2_1 helix (silver, left hatch; nitrogen, right hatch; fluorine, cross-hatched; boron (a) or phosphorus (b), dotted).

ordination, particularly in the presence of the more weakly co-ordinating PhCN ligand. Thus in the structure of complex **6** bis-chelated silver(I) ions are observed which are linked into a one-dimensional polymer through the peripheral bpyz N-donors *via* a trigonal, PhCN-co-ordinated metal centre.

When $MeNO_2$ is used as solvent there is no competition with the bpyz or pyq ligands for co-ordination of the Ag^I and therefore each cation is co-ordinated by chelating N-donors and two monodentate N-donors such that each centre within the polymeric structure adopts an equivalent co-ordination sphere, **1**–**4**.

Bearing this argument in mind it is difficult to rationalise the structure observed in complex **5**, $\{[Ag(bpyz)(MeCN)]BF_4\}_\infty$, in which each silver(I) centre exhibits a five-co-ordinate geometry with a chelating bpyz ligand, two monodentate bpyz ligands and a MeCN ligand all surrounding the same cation. However the construction of a co-ordination polymer is a subtle balance between many energetic forces and not solely dependent upon either the solution phase or solid phase properties of a given system. In the case of **5** it would appear that the energetic preferences of crystalline packing outweigh the advantages of forming $[Ag(MeCN)_4]^+$ cations. This, therefore, suggests that the packing mode adopted by **5** is particularly energetically favourable, leading to its isolation.

Ligand effects. The two ligands, bpyz and pyq, act differently when used to construct co-ordination networks. This can quite readily be rationalised when one considers the steric requirements of the monodentate donors on each ligand. Whereas in bpyz the monodentate N-donors quite readily co-ordinate Ag^I even in the presence of other potential ligands, MeCN in **5** or PhCN in **6**, the sterically hindered monodentate N-donors of pyq cannot compete with MeCN or PhCN donors, resulting in the formation of the discrete non-polymeric species, **7**. In the absence of co-ordinating solvents the relative steric congestion of the monodentate N-donors of pyq results in the formation of compounds **3** and **4** which adopt unusual three-dimensional structures.

Conclusion

In conclusion we have structurally characterised a range of three-, **1**–**4**, two-, **5**, and one-dimensional, **6**, co-ordination polymers and in one case a discrete molecular complex, **7**. The multi-modal ligands allow the construction of unusual co-ordination networks offering the system chemically distinct bridging modes, resulting in the case of **1** and **2** in the formation of a chiral diamondoid network. We have demonstrated that the structural composition of silver(I) co-ordination polymers is not only dependent on ligand functionality but for appropriate systems can also be tuned by anion interactions. The effect of solvent upon the isolated product depends predominantly upon the relative co-ordinative ability of the solvent in question.

Experimental

Infrared spectra were recorded on a Perkin-Elmer 1600 spectrometer (FTIR, samples in KBr discs). Elemental analytical data were obtained by the microanalytical service (Perkin-Elmer 240B analyser) at the University of Nottingham. 2,2′-Bipyrazine was prepared according to the literature method[21] and pyrazino[2,3-*f*]quinoxaline was purchased from Aldrich Chemicals and used without further purification.

Synthesis

$\{[Ag(bpyz)]BF_4\}_\infty$ 1. A solution of $AgBF_4$ (10 mg, 0.05 mmol) in $MeNO_2$ (10 cm^3) was slowly diffused into a solution of 2,2′-bipyrazine (8 mg, 0.05 mmol) in $MeNO_2$ (10 cm^3) to give a homogeneous reaction solution. Diethyl ether vapour was then diffused into the reaction solution affording colourless block crystals. Yield (8 mg, 44%) (Found: C, 27.45; H, 1.87; N, 15.94. Calc. for $C_8H_6AgBF_4N_4$: C, 27.23; H, 1.71; N, 15.88%). IR (KBr)/cm^{-1}: 2923m, 1635w, 1465m, 1383m, 1152m, 1124s, 1083s, 1029s, 1019s, 847m and 430m.

$\{[Ag(bpyz)]PF_6\}_\infty$ 2. This was prepared analogously, replacing $AgBF_4$ with $AgPF_6$. Yield 49% (Found: C, 23.70; H, 1.63; N, 13.22. Calc. for $C_8H_6AgF_6N_4P$: C, 23.38; H, 1.47; N, 13.63%). IR (KBr)/cm^{-1}: 2919s, 2850s, 1560m, 1465m, 1382m, 1152w, 1091m, 1029s, 1019s, 847s, 830s, 559s and 429m.

$\{[Ag(pyq)]BF_4\}_\infty$ 3. A solution of $AgBF_4$ (12 mg, 0.06 mmol) in $MeNO_2$ (10 cm^3) was slowly diffused into a solution of pyq

(10 mg, 0.06 mmol) in $MeNO_2$ (10 cm^3) to give a homogeneous reaction solution. Diethyl ether vapour was then diffused into the reaction solution affording colourless block crystals. Yield (6 mg, 55%) (Found: C, 31.52; H, 2.03; N, 15.26. Calc. for $C_{10}H_6AgBF_4N_4$: C, 31.87; H, 1.60; N, 14.87%). IR (KBr)/cm^{-1}: 2914m, 2852m, 1644m, 1383m, 1260w, 1081s, 1034m and 881w.

{[Ag(pyq)]PF_6}$_\infty$ 4. This was prepared analogously replacing $AgBF_4$ with $AgPF_6$. Yield 46% (Found: C, 27.93; H, 1.70; N, 13.16. Calc. for $C_{10}H_6AgF_6N_4P$: C, 27.61; H, 1.39; N, 12.88%). IR (KBr)/cm^{-1}: 2960w, 2914w, 2842w, 1629w, 1490w, 1383m, 1260w, 1096m, 1029w, 843s and 558s.

{[Ag(bpyz)(MeCN)]BF_4}$_\infty$ 5. This was prepared analogously to {[Ag(bpyz)]BF_4}$_\infty$ but replacing $MeNO_2$ with MeCN. Yield (54%) (Found: C, 30.21; H, 2.09; N, 17.48. Calc. for $C_{10}H_9AgBF_4N_5$: C, 30.49; H, 2.30; N, 17.78%). IR (KBr)/cm^{-1}: 3052w, 3017w, 1490s, 1416m, 1381s, 1289w, 1267m, 1221m, 1088s, 1083s, 1033s, 888s, 875s, 830w, 750m, 521w and 533w.

{[Ag_2(bpyz)$_2$(PhCN)][BF_4]$_2$}$_\infty$ 6. This was prepared analogously to {[Ag(bpyz)]BF_4}$_\infty$ but replacing $MeNO_2$ with PhCN and was isolated as a pale yellow solid. Yield 23% (Found: C, 33.87; H, 2.06; N, 15.35. Calc. for $C_{23}H_{17}Ag_2B_2F_8N_9$: C, 34.16; H, 2.12; N, 15.59%). IR (KBr)/cm^{-1}: 2919m, 2850m, 1493m, 1419w, 1384s, 1265m, 1218w, 1084s, 1047s, 885s, 749w, 440m and 420w.

[Ag(pyq)$_2$]BF_4 7. This was prepared analogously to {[Ag(pyq)]BF_4}$_\infty$ replacing $MeNO_2$ with MeCN (**7a**) or PhCN (**7b**) and was isolated as a pale yellow solid. Yield 36% (Found: C, 42.71; H, 1.54; N, 19.76. Calc. for $C_{20}H_{12}AgBF_4N_8$: C, 42.97; H, 2.16; N, 20.04%). IR (KBr)/cm^{-1}: 3062w, 2919w, 2847w, 1629w, 1490s, 1383s, 1260m, 1214w, 1081s, 1055s, 871m, 743w and 441m.

Crystals of bpyz of suitable quality for single crystal X-ray diffraction studies were grown by diffusion of diethyl ether vapour into a nitromethane solution of the compound. Crystals of pyq were grown by slow evaporation of a nitromethane solution of the compound.

Crystallography

All single crystal X-ray experiments were performed on either a Stoë Stadi-4 four-circle diffractometer (bpyz, **1**, **5**) or Bruker AXS SMART CCD detector diffractometer (pyq, **2**, **3**, **6**, **7a**, **7b**) both equipped with an Oxford Cryosystems open flow cryostat[22] [graphite monochromated Mo-Kα radiation (λ = 0.71073 Å); ω–θ (bpyz, **1**,**5**) or ω scans (pyq, **2**, **3**, **6**, **7a**, **7b**)]. Absorption corrections were applied either by a semi-empirical approach for complexes **2**, **3**, **6**, **7a**, **7b**, numerically for **1** or using ψ scans **5**. None was made in the cases of bpyz and pyq. Other details of crystal data, data collection and processing are given in Table 4. All structures were solved with direct methods using SHELXS 97[23] and all non-H atoms were located using subsequent Fourier-difference methods.[24] In all cases hydrogen atoms were placed in calculated positions and thereafter allowed to ride on their parent atoms. Complex **3** was found to exhibit disorder in both the BF_4^- anions and nitromethane solvent molecules. The fluorine atoms of two BF_4^- anions were modelled isotropically over two sets of sites (occupancy 0.6, 0.4). Two further BF_4^- anions were found to be disordered over an inversion centre and thus half-occupied. One $MeNO_2$ molecule was similarly refined as half-occupied in close proximity to a half-occupied BF_4^- anion. The largest residual density (1.8 e $Å^{-3}$) was sited near a disordered BF_4^- anion. For **6** the fluorine atoms of one BF_4^- anion were disordered and modelled isotropically over three sites (occupancy 0.40, 0.35, 0.25) and for the other BF_4^- anion three of the fluorine atoms were each modelled over two sites (occupancy 0.65, 0.35). The assignment

Table 4 Crystallographic data summary

	bpyz	pyq	**1**[15]	**2**	**3**	**5**[15]	**6**	**7a**	**7b**
Empirical formula	$C_8H_6N_4$	$C_{10}H_6N_4$	$C_{10}H_{12}AgBF_4N_6O_4$	$C_{10}H_{12}AgF_6N_6O_4P$	$C_{11.5}H_{10.5}AgBF_4N_{5.5}O_3$	$C_{10}H_9AgBF_4N_5$	$C_{23}H_{17}Ag_2B_2F_8N_9$	$C_{20}H_{12}AgBF_4N_8$	$C_{20}H_{12}AgBF_4N_8$
M	158.17	182.19	474.94	533.10	468.43	393.90	808.81	559.06	559.06
Crystal system	Triclinic	Orthorhombic	Tetragonal	Tetragonal	Monoclinic	Monoclinic	Monoclinic	Monoclinic	Monoclinic
Space group	$P\bar{1}$	$P2_12_12_1$	$P4_32_12$	$P4_32_12$	$P2_1/n$	$P2_1/n$	$P2_1/c$	$C2/c$	$C2/c$
a/Å	3.686(5)	3.7611(8)	11.396(7)	12.828(2)	16.981(2)	7.326(3)	11.410(3)	16.898(2)	9.375(2)
b/Å	5.290(6)	8.271(2)	—	—	15.166(2)	18.423(6)	14.379(3)	7.2786(6)	15.608(3)
c/Å	9.470(14)	26.110(5)	13.913(9)	11.020(1)	19.436(2)	10.218(4)	16.153(4)	17.146(2)	13.999(3)
α/°	102.43(11)	—	—	—	—	—	—	—	—
β/°	92.78(11)	—	—	—	95.825(1)	100.35(4)	91.497(4)	111.751(2)	107.37(3)
γ/°	100.93(9)	—	—	—	—	—	—	—	—
U/Å^3	176.3(4)	812.2(3)	1807(2)	1813.4(4)	4979.5(10)	1356.7(9)	2649.3(11)	1958.7(4)	1955.0(7)
Z	1	4	4	4	12	4	2	4	4
T/K	150(2)	150(2)	150(2)	150(2)	150(2)	150(2)	150(2)	150(2)	150(2)
μ/mm^{-1}	0.099	0.097	1.183	1.290	1.281	1.531	1.570	1.096	1.098
Reflections collected	688	1197	1595	2228	12036	2384	6338	2332	2292
Unique reflections	618	1197	1391	2054	7692	1794	5219	2239	2116
Final *R*1 [$F > 4\sigma(F)$]	0.0405	0.0485	0.0549	0.0241	0.0558	0.0531	0.0305	0.0215	0.0274
*wR*2 (all data)	0.1182	0.1290	0.1262	0.0578	0.1818	0.0913	0.0828	0.0603	0.0727

of the absolute structures for **1** and **2** was confirmed by the refinement of Flack enantiopole parameters to values of −0.12(12) and 0.08(3), respectively.[25]

X-Ray diffraction experiments on single crystals of compound **4** allowed not only determination of the unit cell and unambiguous determination of the space group (monoclinic; $a = 17.1722(13)$, $b = 15.454(11)$, $c = 20.1874(15)$ Å, $\beta = 96.209°$, $V = 5325.89$ Å^3, space group $P2_1/n$ but also refinement of the $[Ag(pyq)^+]_\infty$ cationic framework. However severe disorder of PF_6^- anions and $MeNO_2$ solvent molecules could not adequately be modelled, leaving residual electron density peaks of up to 3.75 e Å^{-3}.

CCDC reference number 186/2024.

See http://www.rsc.org/suppdata/dt/b0/b003202f/ for crystallographic files in .cif format.

Acknowledgements

We thank the University of Nottingham (J. E. B. N.) and the EPSRC for support.

References

1 S. R. Batten and R. Robson, *Angew. Chem.*, *Int. Ed.*, 1998, **37**, 1460.
2 A. J. Blake, N. R. Champness, P. Hubberstey, W.-S. Li, M. Schröder and M. A. Withersby, *Coord. Chem. Rev.*, 1999, **183**, 117.
3 P. K. Bowyer, K. A. Porter, A. D. Rae, A. C. Willis and S. B. Wild, *Chem. Commun.*, 1998, 1153; S. R. Batten, B. F. Hoskins and R. Robson, *Angew. Chem.*, *Int. Ed. Engl.*, 1997, **36**, 636; C. Kaes, M. W. Hosseini, C. E. F. Rickard, B. W. Skelton and A. H. White, *Angew. Chem.*, *Int. Ed.*, 1998, **37**, 920; B. Wum, W.-J. Zhang, S.-Y. Yu and X.-T. Wu, *J. Chem. Soc.*, *Dalton Trans.*, 1997, 1795; O. J. Gelling, F. van Bolhuis and B. L. Feringa, *J. Chem. Soc.*, *Chem. Commun.*, 1991, 917; Y. Dai, T. J. Katz and D. A. Nichols, *Angew. Chem.*, *Int. Ed. Engl.*, 1996, **35**, 2109; K. Biradha, C. Seward and M. J. Zaworotko, *Angew. Chem.*, *Int. Ed.*, 1999, **38**, 492; T. Ezuhara, K. Endo and Y. Aoyama, *J. Am. Chem. Soc.*, 1999, **121**, 3279.
4 H.-P. Wu, C. Janiak, L. Uehlin, P. Klüfers and P. Mayer, *Chem. Commun.*, 1998, 2637; H.-P. Wu, C. Janiak, G. Rheinwald and H. Lang, *J. Chem. Soc.*, *Dalton Trans.*, 1999, 183; C. Janiak, L. Uehlin, H.-P. Wu, P. Klüfers, H. Piotrowski and T. G. Scharmann, *J. Chem. Soc.*, *Dalton Trans.*, 1999, 3121.
5 For examples see O. M. Yaghi and G. Li, *Angew. Chem.*, *Int. Ed. Engl.*, 1995, **34**, 207; R. W. Gable, B. F. Hoskins and R. Robson, *J. Chem. Soc.*, *Chem. Commun.*, 1990, 1677; J. Lu, T. Paliwala, S. C. Lim, C. Yu, T. Niu and A. J. Jacobson, *Inorg. Chem.*, 1997, **36**, 923; S. W. Keller and S. Lopez, *J. Am. Chem. Soc.*, 1999, **121**, 6306.
6 For examples see H. Gudbjartson, K. Biradha, K. M. Poirier and M. J. Zaworotko, *J. Am. Chem. Soc.*, 1999, **121**, 2599; B. F. Abrahams, P. A. Jackson and R. Robson, *Angew. Chem.*, *Int. Ed.*, 1998, **37**, 2656; L. Carlucci, G. Ciani, P. Macchi and D. M. Proserpio, *Chem. Commun.*, 1998, 1837.
7 A. J. Blake, N. R. Champness, S. S. M. Chung, W.-S. Li and M. Schröder, *Chem. Commun.*, 1997, 1005; A. J. Blake, N. R. Champness, A. N. Khlobystov, D. A. Lemenovski, W.-S. Li and M. Schröder, *Chem. Commun.*, 1997, 1339; O. R. Evans, R.-G. Xiong, Z. Wang, G. K. Wong and W. Lin, *Angew. Chem.*, *Int. Ed.*, 1999, **38**, 536; S. Lopez, M. Kahraman, M. Harmata and S. W. Keller, *Inorg. Chem.*, 1997, **36**, 6138; K. A. Hirsch, D. Venkataraman, S. R. Wilson, J. S. Moore and S. Lee, *J. Chem. Soc.*, *Chem. Commun.*, 1995, 2199; L. R. MacGillivray, S. Subramanian and M. J. Zaworotko, *J. Chem. Soc.*, *Chem. Commun.*, 1994, 1325; L. Carlucci, G. Ciani, D. M. Proserpio and A. Sironi, *J. Chem. Soc.*, *Chem. Commun.*, 1994, 2755.
8 K. A. Hirsch, S. R. Wilson and J. S. Moore, *Chem. Eur. J.*, 1997, **3**, 765.
9 O. M. Yaghi, H. Li, C. Davis, D. Richardson and T. L. Groy, *Acc. Chem. Res.*, 1998, **31**, 474.
10 For examples see S. R. Batten, B. F. Hoskins and R. Robson, *Chem. Eur. J.*, 2000, **6**, 156 and refs. therein.
11 M. A. Withersby, A. J. Blake, N. R. Champness, P. A. Cooke, P. Hubberstey and M. Schröder, *J. Am. Chem. Soc.*, 2000, **122**, 4044. B. F. Abrahams, M. J. Hardie, B. F. Hoskins, R. Robson and E. E. Sutherland, *J. Chem. Soc.*, *Chem. Commun.*, 1994, 1049; B. F. Abrahams, S. R. Batten, M. J. Grannas, H. Hamit, B. F. Hoskins and R. Robson, *Angew. Chem.*, *Int. Ed.*, 1999, **38**, 1475.
12 L. Carlucci, G. Ciani, P. Macchi, D. M. Proserpio and S. Rizzato, *Chem. Eur. J.*, 1999, **5**, 237; M. A. Withersby, A. J. Blake, N. R. Champness, P. Hubberstey, W.-S. Li and M. Schröder, *Angew. Chem.*, *Int. Ed. Engl.*, 1997, **36**, 2327; M. A. Withersby, A. J. Blake, N. R. Champness, P. A. Cooke, P. Hubberstey, W.-S. Li and M. Schröder, *Cryst. Eng.*, 1999, **2**, 123; K. A. Hirsch, S. R. Wilson and J. S. Moore, *Inorg. Chem.*, 1997, **36**, 2960; D. Venkataraman, S. Lee, J. S. Moore, P. Zhang, K. A. Hirsch, G. B. Gardner, A. C. Covey and C. L. Prentice, *Chem.Mater.*, 1996, **8**, 2030.
13 A. J. Blake, N. R. Champness, P. A. Cooke and J. E. B. Nicolson, *Chem. Commun.*, 2000, 665.
14 M. H. Chisholm, J. C. Huffman, I. P. Rothwell, P. G. Bradley, N. Kress and W. H. Woodruff, *J. Am. Chem. Soc.*, 1981, **103**, 4945.
15 S. Nishigaki, H. Yoshioka and K. Nakatsu, *Acta Crystallogr.*, *Sect. B*, 1978, **34**, 875.
16 A. L. Spek, PLATON, *Acta Crystallogr.*, *Sect. A*, 1990, **46**, C-34.
17 K. A. Hirsch, S. R. Wilson and J. S. Moore, *Inorg. Chem.*, 1997, **36**, 2960; L. Carlucci, G. Ciani, D. M. Proserpio and A. Sironi, *Angew. Chem.*, *Int. Ed. Engl.*, 1995, **34**, 1895; G. K. H. Shimizu, G. D. Enright, C. I. Ratcliffe, J. A. Ripmeester and D. D. M. Rayner, *Angew. Chem.*, *Int. Ed. Engl.*, 1997, **37**, 1407.
18 J. Nasielski, R. Nasielski-Hinkens, S. Heilporn, C. Rypens and J. P. Declerq, *Bull. Chem. Soc. Belg.*, 1988, **97**, 983.
19 D. M. P. Mingos and A. L. Rohl, *Inorg. Chem.*, 1991, **30**, 3769; D. M. P. Mingos and A. L. Rohl, *J. Chem. Soc.*, *Dalton Trans.*, 1991, 3419.
20 K. Nilsson and A. Oskarsson, *Acta Chem. Scand.*, *Ser. A*, 1984, **38**, 79.
21 R. J. Crutchley and A. B. P. Lever, *Inorg. Chem.*, 1982, **21**, 2276.
22 J. Cosier and A. M. Glazer, *J. Appl. Crystallogr.*, 1986, **19**, 105.
23 G. M. Sheldrick, SHELXS 97, University of Göttingen, 1997.
24 G. M. Sheldrick, SHELXL 97, University of Göttingen, 1997.
25 H. D. Flack, *Acta Crystallogr.*, *Sect. A*, 1983, **39**, 876.